

# Multiobjective Optimal Suspension Control to Achieve Integrated Ride and Handling Performance

Jianbo Lu, *Member, IEEE*, and Mark DePoyster

**Abstract**—Multiobjective optimal control strategy is pursued here for finding feedback control laws used in controlled suspensions for automotive vehicles. The balanced vehicle ride and handling performances are the main concern of this paper. The ride performance (car body performance) is characterized by an  $H_2$  system norm, and the handling performance (wheel performance) is characterized by an  $H_\infty$  system norm, and the control method optimizes the mixed  $H_2/H_\infty$  performances. The  $H_2$  and  $H_\infty$  system norms used in the mixed  $H_2/H_\infty$  performance optimization are scaled by the corresponding open-loop norms such that the relative importance of the individual variables can be reflected in the performance index for the vector variables. The comparison between passive and controllable suspensions shows in simulation the advantages of this optimal control strategy. The simulation result also shows that the invariant point for controlled suspensions in the quarter car case exists in the seven degree-of-freedom model. The control scheme was tested and validated for a test vehicle, current paper only shows the simulation work.

**Index Terms**—Mixed  $H_2/H_\infty$  control, vehicle handling performance, vehicle ride performance, vehicle suspension control.

## I. INTRODUCTION

THE COMPUTER-CONTROLLED suspensions for transportation have been studied for decades. Many control strategies have been proposed. A good summary can be found in [11] and [12] for automotive applications. Various strategies which have been pursued include different modern linear and nonlinear control methods. For example, [1] considers adaptive control, [2]–[4] and [7] use linear quadratic Gaussian (LQG) strategy for automotive vehicles, [14] uses  $H_\infty$  control to an active suspension for railway vehicles. Other strategies (for example, preview control) can also be found in the literature.

The literature in this topic is very rich, however, most of the work is focusing on controlling vehicle vertical dynamics of two degrees of freedom (quarter-car model) or of four degrees of freedom (half-car model). A handful few researched how to control vehicle vertical dynamics of seven degree-of-freedom (full-car model); for example, see [2]–[4], [7], and [8]. Another bias is emphasizing ride performance (good control of vehicle body motions) and in general paying insufficient attention to

vehicle wheel motions. In practice, the interaction between the wheels and road surfaces plays significant role for a vehicle to maximize its stability during handling maneuvers, to reduce stopping distance and to reduce road damage (especially for heavy trucks). Current advances in system-level controls demands much more stringent performances for vehicle wheel motions than before. For example, maintaining as small tire dynamic normal force (excursions from nominal normal force) as possible is pursued for many integrated vehicle control systems on top of the ride comfort requirement. This motivates the main theme of this paper: how to design algorithms for controllable suspensions to achieve desired vehicle body and wheel performances, or say, to achieve a balanced ride and handling performance.

Recently, mass production of controllable suspensions in automotive applications is increasingly getting attention from both auto makers and auto parts suppliers. Many auto makers and suppliers are working together to offer controlled suspension as an option for high-end passenger cars. One of such example is the semiactive suspension called continuous variable real-time damper (CVRTD), developed at Delphi Automotive Systems, which is now commercially available in several vehicle platforms. This commercial need revives development activities in controlled suspensions, for example at Delphi Automotive Systems. Current control strategies used in Delphi's CVRTD system are mainly based on the well-known sky-hook damping [12] and certain wheel motion control, together with sophisticated nonlinear gain scheduling schemes. In order to achieve desired performances with respect to all driving conditions, CVRTD control algorithms involved hundreds of calibration parameters and possible patches. The strategy has been successfully proven in vehicles.

In order to increase application efficiency, primarily tuning control algorithms in computer simulation environment could significantly reduce the expensive in-vehicle tuning effort. This tuning strategy uses field tests as a supplement, i.e., as a validation tool and for small scale tuning. Along this line of thinking, the clean sheet approaches have been sought as a potential alternative in the future at Delphi Automotive Systems. The clean sheet approach aims to solve the potential performance degradation upfront, using intensive computer simulation as a design/validation tool before in-vehicle tuning is conducted. The current paper summarized one of these efforts. What we want to accomplish here is to tune a CVRTD algorithm by utilizing as much simulation as possible for achieving balanced vehicle body and wheel performance. The strategy used here is the so-called mixed  $H_2/H_\infty$  optimal control method. This mixed  $H_2/H_\infty$  control has been studied a great deal during

Manuscript received July 6, 2001; revised November 6, 2001. Manuscript received in final form February 4, 2002. Recommended by Associate Editor Y. Jin.

J. Lu was with the Engineering Technical Center of Engine Management and Chassis Systems, Delphi Automotive Systems, Dayton, OH 45401 USA. He is now with Research and Vehicle Technology, Ford Motor Company, Dearborn, MI 48124 USA (e-mail: jlu10@ford.com).

M. DePoyster is with Engine Management and Chassis Systems, Delphi Automotive Systems, Dayton, OH 45401 USA.

Digital Object Identifier 10.1109/TCST.2002.804121

last decade (for example, see [5], [17], [16]). Using the linear matrix inequality (short to LMI) studied in [6], [18], this mixed  $H_2/H_\infty$  control problem can be solved very efficiently. A software toolbox for implementing the convex algorithms using LMI is now available for Matlab users (see [9] for detail). This toolbox is called LMI Control Toolbox. Notice that [19] studies a “multiobjective approach” in designing an  $H_2$  or an  $H_\infty$  suspension control law for a quarter-car model, which is different from the mixed  $H_2/H_\infty$  optimization approach here. Over there, the weights used to reflect the individual performance of the ride comfort, the road-holding and the rattle-space are sought based on a local optimization algorithm and the weights are then used to construct the final  $H_2$  (or  $H_\infty$ ) control law.

This paper is organized as follows. Section II considers the matrix form of the vertical vehicle dynamics. A linear transformation is used to transfer the equation of motion to the form good for control design. A brief discussion about vehicle performance evaluations is included in Section III. Section IV includes control design strategy and method. A numerical example is included in Section V. Section VI concludes this paper.

The following notations are used in this paper. For a matrix  $M$ ,  $M > 0$  means that the matrix is positive definite or all its eigenvalues are positive numbers;  $M < 0$  means  $-M > 0$ ;  $M'$  denotes the matrix transpose;  $M^+$  denotes the matrix pseudoinverse. For a transfer matrix  $T(s)$ ,  $T^*(j\omega)$  means the conjugate transpose of the frequency response  $T(j\omega)$ ,  $\bar{\sigma}(T(j\omega))$  is the largest singular value of the frequency response  $T(j\omega)$  evaluated at frequency  $\omega$ .  $\mathbb{R}$  is the set of all real numbers.  $\text{diag}(\cdot)$  formulates a diagonal matrix.

## II. VERTICAL VEHICLE DYNAMICS

Assume a vehicle under study is driven in a straight road in a steady-state condition, i.e., with constant thrust and without brake action. In this case, the vertical dynamics of the vehicle include the car body heave, roll, and pitch motions, and the four wheel bounce motions. This is a typical seven degree-of-freedom characterization of the vertical dynamics used for controlled suspensions. If both the longitudinal and lateral motions of the vehicle are excessive, further degrees of freedom must be included in order to provide a reasonable model. Three more degrees of freedom are needed: the vehicle yaw, lateral, and longitudinal motion. That is, the resultant system should be characterized by ten degrees of freedom. Although this ten degree-of-freedom dynamics is useful in integrated vehicle dynamics control, this paper focuses on the seven degree-of-freedom dynamics. The extension of combining the current approach with other control strategies in controlling ten degrees of freedom of a vehicle will be studied separately.

Notice that in Fig. 1, we assume that the spring, the damper, the wheel at each of the four corners of the vehicle and the sensor used to measure the relative position between the two ends of the suspension spring are collocated. Although this is different from the real configuration where noncollocation

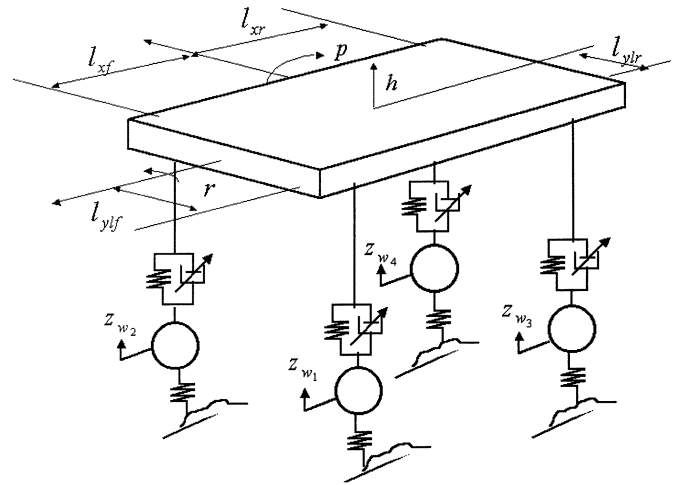


Fig. 1. A vertical vehicle model of seven degrees of freedom.

spring, damper and sensor are used, transformations can be used to convert the noncollocated configurations to the collocated configurations without loss of generality.

Let

$$z_w = \begin{bmatrix} z_{w_1} \\ z_{w_2} \\ z_{w_3} \\ z_{w_4} \end{bmatrix}$$

be the displacement vector whose  $i$ th element denotes the absolute displacement of the  $i$ th wheel of the vehicle, where  $i = 1, 2, 3,$  and  $4$  corresponds to the left-front, right-front, left-rear, and right-rear wheels.

The body motion vector is defined as

$$q = \begin{bmatrix} h \\ r \\ p \end{bmatrix}$$

where  $h$  is the heave displacement of the center of gravity of the car body (sprung mass),  $r$  is the car body's roll angle, and  $p$  is the car body's pitch angle. Both  $r$  and  $p$  are the global angular displacements with respect to a perfect flat road surface or the sea level.

Denote

$$z_b = \begin{bmatrix} z_{b_1} \\ z_{b_2} \\ z_{b_3} \\ z_{b_4} \end{bmatrix}$$

as the vector whose  $i$ th element is the vertical displacement of the car body in the  $i$ th corner, where  $i = 1, 2, 3,$  and  $4$  corresponds to the left-front, right-front, left-rear, and the right-rear corners where the suspensions are connected.

Let  $H$  be the transformation matrix relating body motion vector  $q$  to the corner position vector  $z_b$ , i.e.,

$$z_b = Hq.$$

For the collocated configuration in Fig. 1,  $H$  can be calculated using vehicle geometry parameters as in the following:

$$H = \begin{bmatrix} 1 & l_{y1f} & -l_{xf} \\ 1 & -l_{y1f} & -l_{xf} \\ 1 & l_{y1r} & l_{xr} \\ 1 & -l_{y1r} & l_{xr} \end{bmatrix}$$

where  $l_{xf}$  and  $l_{xr}$  are the distances from the front and rear axle to car body center of gravity, respectively,  $l_{y1f}$  and  $l_{y1r}$  are half of the front and rear wheel tracks.

The relative positions of the suspensions at the left-front, the right-front, the left-rear, and the right-rear corners are denoted as

$$z_{rp} = \begin{bmatrix} z_{rp1} \\ z_{rp2} \\ z_{rp3} \\ z_{rp4} \end{bmatrix}$$

which can be computed from  $z_b$  and  $z_w$

$$z_{rp} = z_b - z_w. \quad (1)$$

Let  $S$  be the total suspension force vector, which is a nonlinear function of the active control variable  $u$ , the relative position vector  $z_{rp}$  and the relative velocity vector  $\dot{z}_{rp}$

$$S = S(u, z_{rp}, \dot{z}_{rp}). \quad (2)$$

Using this suspension force  $S$ , the equation of motion for the car body can be expressed as

$$\begin{aligned} M_s \ddot{h} &= [1 \ 1 \ 1 \ 1] S(u, z_{rp}, \dot{z}_{rp}) \\ I_{xx} \ddot{r} &= [l_{y1f} \ -l_{y1f} \ l_{y1r} \ -l_{y1r}] S(u, z_{rp}, \dot{z}_{rp}) \\ I_{yy} \ddot{p} &= [-l_{xf} \ -l_{xf} \ l_{xr} \ l_{xr}] S(u, z_{rp}, \dot{z}_{rp}) \end{aligned} \quad (3)$$

where  $M_s$  is the sprung mass,  $I_{xx}$  and  $I_{yy}$  are the roll and pitch moments of inertia of the car body, respectively.

Let

$$M_b = \text{diag}(M_s, I_{xx}, I_{yy})$$

then (3) can be rewritten as the following matrix form:

$$M_b \ddot{q} = H' S(u, z_{rp}, \dot{z}_{rp}). \quad (4)$$

If we define

$$\begin{aligned} M_w &= \text{diag}(M_{w1}, M_{w2}, M_{w3}, M_{w4}) \\ K_t &= \text{diag}(K_{t1}, K_{t2}, K_{t3}, K_{t4}) \end{aligned}$$

where  $M_{wi}$  is the unsprung mass at the  $i$ th corner,  $K_{ti}$  is the  $i$ th tire stiffness, then the wheel equations of motion can be written as the following matrix form:

$$M_w \ddot{z}_w = -S(u, z_{rp}, \dot{z}_{rp}) - K_t(z_w - w) \quad (5)$$

where  $w$  is the road profile vector. Equations (4) and (5) consist of the mathematical description of a seven degree-of-freedom vehicle vertical dynamics.

Using small motion assumption, the suspension forces in (2) can be linearized around the steady-state operation point. That is,  $S(u, z_{rp}, \dot{z}_{rp})$  can be approximated as a linear function of the relative positions, the relative velocities and the control variable

$$S = -K_s z_{rp} - C_s \dot{z}_{rp} + u \quad (6)$$

where  $u$  could be the active suspension force or the semiactive suspension damping force, and

$$\begin{aligned} K_s &= \text{diag}(K_{s1}, K_{s2}, K_{s3}, K_{s4}) \\ C_s &= \text{diag}(C_{s1}, C_{s2}, C_{s3}, C_{s4}) \end{aligned}$$

with  $K_{si}$  as the passive suspension spring rate at the  $i$ th corner, and  $C_{si}$  as the passive damping rate at the  $i$ th corner.

Plugging (6) into (4) and (5) leads to the following matrix form of the linearized vehicle vertical dynamics:

$$\begin{aligned} M_b \ddot{q} &= -H' K_s (Hq - z_w) - H' C_s (H\dot{q} - \dot{z}_w) + H' u \\ M_w \ddot{z}_w &= K_s (Hq - z_w) + C_s (H\dot{q} - \dot{z}_w) - u - K_t (z_w - w). \end{aligned} \quad (7)$$

If we introduce a new variable

$$\hat{z} = \begin{bmatrix} q \\ z_w \end{bmatrix}$$

then (7) can be rewritten as

$$M \ddot{\hat{z}} + D \dot{\hat{z}} + K \hat{z} = E_1 w + E_2 u \quad (8)$$

where

$$\begin{aligned} M &= \begin{bmatrix} M_b & 0 \\ 0 & M_w \end{bmatrix} \\ K &= \begin{bmatrix} H' K_s H & H' K_s \\ -K_s H & K_t + K_s \end{bmatrix} \\ D &= \begin{bmatrix} H' C_s H & -H' C_s \\ -C_s H & C_s \end{bmatrix} \\ E_1 &= \begin{bmatrix} 0 \\ K_t \end{bmatrix} \\ E_2 &= \begin{bmatrix} H' \\ -I \end{bmatrix}. \end{aligned}$$

If we further define

$$\hat{x} = \begin{bmatrix} \hat{z} \\ \dot{\hat{z}} \end{bmatrix}.$$

Equation (8) can be expressed in the following state-space form:

$$\dot{\hat{x}} = \hat{A} \hat{x} + \hat{B}_1 w + \hat{B}_2 u \quad (9)$$

where

$$\begin{aligned} \hat{A} &= \begin{bmatrix} 0 & I \\ -M^{-1}K & -M^{-1}D \end{bmatrix} \\ \hat{B}_1 &= \begin{bmatrix} 0 \\ M^{-1}E_1 \end{bmatrix} \\ \hat{B}_2 &= \begin{bmatrix} 0 \\ M^{-1}E_2 \end{bmatrix}. \end{aligned}$$

Notice that  $\hat{A}$  is invertible if and only if the  $K$  matrix in the equation of motion (8) is invertible. If  $K$  is invertible, the inverse of  $\hat{A}$  can be written as

$$\hat{A}^{-1} = \begin{bmatrix} -K^{-1}D & -K^{-1}M \\ I & 0 \end{bmatrix}. \quad (10)$$

Since any nonsingular and linear transformation does not change system dynamics, we want to change (9) from using  $w$  as disturbance to using  $\dot{w}$  as disturbance. The following theorem discusses this.

*Theorem 1:* If  $K$  matrix in the equation of motion (8) is invertible, then there exist state transformations

$$x = L \left( \hat{x} + \begin{bmatrix} K^{-1}E_1 \\ 0 \end{bmatrix} w \right)$$

for any nonsingular matrix  $L$  with proper dimension, such that (9) can be changed to

$$\dot{x} = Ax + B_1\dot{w} + B_2u. \quad (11)$$

*Proof:* Consider the transformation

$$x = L\hat{x} - Nw. \quad (12)$$

Plugging (12) into (9) leads to

$$\dot{x} = L\hat{A}L^{-1}x + L(\hat{A}L^{-1}N + \hat{B}_1)w - N\dot{w} + L\hat{B}_2u. \quad (13)$$

since the inverse of  $\hat{A}$  in (9) exists if  $K$  is invertible. Hence, we can eliminate  $w$  term in (13) by choosing

$$N = -L\hat{A}^{-1}\hat{B}_1 = L \begin{bmatrix} K^{-1}E_1 \\ 0 \end{bmatrix}$$

i.e., (13) can be simplified to (11) with

$$\begin{aligned} A &= L\hat{A}L^{-1} \\ B_1 &= -N \\ B_2 &= L\hat{B}_2. \end{aligned}$$

Hence, the theorem is true.

The above result shows that the existence of linear transformations which can alter the state-space description of the vehicle dynamics from using road profile  $w$  as disturbance to using the road profile velocity  $\dot{w}$  as disturbance. One advantage of using  $\dot{w}$  to replace  $w$  is due to the consideration that  $\dot{w}$  has richer dynamic components than  $w$ . Therefore,  $\dot{w}$  is much closer to white noise than  $w$  for actual road profiles, see [11] and [12] for more discussion. Since the state-space control algorithms considered here is a model-based control strategy, a Kalman-like state estimation or observer is inevitably embedded in the control algorithm. This state estimator typically works well if the system disturbance is close to white noise process.

Now let us consider choosing state transformation. The system states assembling (9) uses  $q$ ,  $z_w$ ,  $\dot{q}$ ,  $\dot{z}_w$  as the system states. There are infinity numbers of ways to choose other combinations. In order to maximize the use of the measured sensor signals, it is possible to include  $z_{rp}$  as part of the states. For example, we could choose 1)  $z_{rp}$ ,  $\dot{z}_{rp}$ ,  $z_w$ ,  $\dot{z}_w$  or 2)  $z_{rp}$ ,  $\dot{z}_{rp}$ ,  $q$ ,  $\dot{q}$ . State set 1) actually includes 16 variables, which means two variables are redundant. State set 2) seems okay, but does introduce more disturbance terms ( $w$ ,  $\dot{w}$ ,  $\ddot{w}$  might appear in the system description). In the following, instead of directly using  $z_{rp}$  as part of system states, a  $3 \times 1$  vector  $\theta$  will be generated from this  $4 \times 1$  vector  $z_{rp}$ .

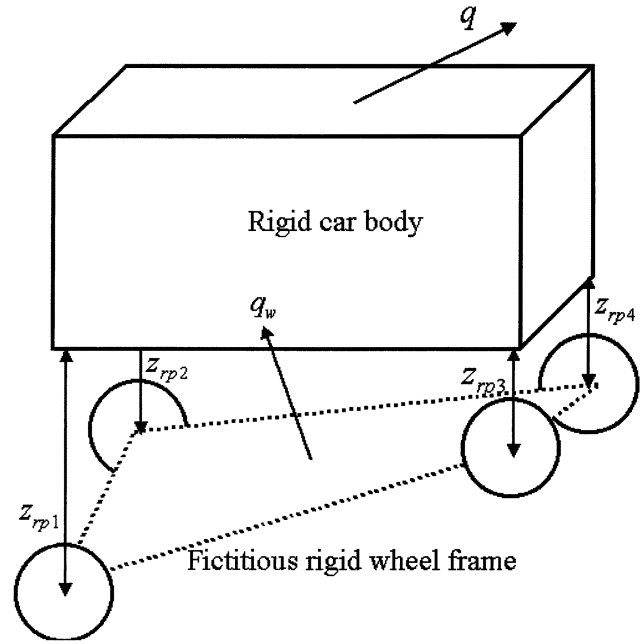


Fig. 2. Motion vector  $q_w$  of the heave, roll and pitch for the fictitious wheel frame, and the motion vector  $q$  for the car body.

Let us use a fictitious rigid frame to connect the four wheels of the vehicle, i.e., constraints posed on the four independent wheels such that they move together in a rigid fashion (see Fig. 2). This fictitious rigid wheel frame has heave, roll, and pitch angular motions. Denote them as

$$q_w = \begin{bmatrix} h_w \\ r_w \\ p_w \end{bmatrix}$$

which can be uniquely determined from the wheel displacement  $z_w$ . The difference between the heave, roll, and pitch of the car body and the heave, roll, and pitch of this fictitious wheel frame is called the relative heave, roll, and pitch. They are defined as the following vector variable:

$$\theta = q - q_w$$

and the relative position  $z_{rp}$  can be expressed as

$$z_{rp} = H\theta. \quad (14)$$

Since the actual wheels are moved independently, (14) is generally not true. Considering the fact that any motion can be decomposed as rigid motion and a nonrigid motion, the actual wheel motion variables might be written as

$$z_w = z_{w_{\text{rigid}}} + z_{w_{\text{nonrigid}}}. \quad (15)$$

with

$$z_{w_{\text{rigid}}} = Hq_w.$$

Hence, generally speaking, we have

$$z_{rp} = H\theta - z_{w_{\text{nonrigid}}}. \quad (16)$$

The question now is how to compute  $z_{w_{\text{nonrigid}}}$  and  $q_w$ . Since  $H$  is a nonsquare matrix, by using a pseudoinverse,  $z_w$  can be decomposed along the direction defined by  $H$

$$z_w = HH^+z_w + (I - HH^+)z_w. \quad (17)$$

By comparing (15) and (17), we have

$$q_w = H^+ z_w, \quad z_{w_{\text{nonrigid}}} = (I - HH^+) z_w. \quad (18)$$

With decomposition (18),  $z_{rp}$  in (16) can be rewritten as

$$\begin{aligned} z_{rp} &= H(q - H^+ z_w) + (HH^+ - I)z_w \\ &= H\theta + (HH^+ - I)z_w. \end{aligned} \quad (19)$$

Considering

$$H^+ HH^+ = H^+$$

(19) implies

$$H^+(z_{rp} - H\theta) = 0$$

i.e., the  $3 \times 1$  vector  $\theta$  is linearly related to the  $4 \times 1$  vector  $z_{rp}$ .

Now, we include  $\theta$  as part of the new states and the total state vector is defined as

$$x = \begin{bmatrix} \theta \\ z_w \\ \dot{q} \\ \dot{z}_w \end{bmatrix} - Nw \in \mathbb{R}^{14}$$

where

$$\begin{bmatrix} \theta \\ z_w \\ \dot{q} \\ \dot{z}_w \end{bmatrix} = L\hat{x} \quad (20)$$

and the transformation matrices  $L$  and  $N$  can be expressed as

$$\begin{aligned} L &= \begin{bmatrix} I & -H^+ & 0 & 0 \\ 0 & I & 0 & 0 \\ 0 & 0 & I & \\ 0 & 0 & 0 & I \end{bmatrix} \\ N &= \begin{bmatrix} \begin{bmatrix} I & -H^+ \\ 0 & I \end{bmatrix} & K^{-1}E_1 \\ & 0 \end{bmatrix}. \end{aligned}$$

### III. VEHICLE PERFORMANCE

Generally speaking, a vehicle's ride comfort (body performance) and its road holding capability (wheel performance) are conflicting objectives [12]. Ride comfort requires that the car body achieves small acceleration levels and ideally to achieve zero car body accelerations. Therefore, the body performance requires minimizing the acceleration levels for the car body's heave, pitch, and roll motions with respect to typical road profiles. We should call this body regulation performance (BRP).

The handling performance, or the wheel performance implies that the wheel normal forces are kept as constant as possible. Physically, this means that wheels follow well with the road profiles, so as to achieve as constant tire deflection as possible. We should call this desired wheel behavior as wheel following performance (WFP).

The performance variables for BRP can be chosen as the acceleration of the heave, roll, and pitch accelerations  $\ddot{q}$ . The tire deflection derivative is one possible variable to measure WFP due to the fact that the small tire deflection derivatives imply

small variations of the tire deflections. Notice that the so-called warped pattern leads to

$$\dot{z}_{td} = 0$$

and

$$z_{td} \neq 0$$

however, the warped pattern rarely happens in reality.

In order to mathematically characterize BRP and WFP, both time and frequency responses can be used. The traditional frequency response is mainly dealing with a single-input–single-output system. In order to evaluate performances for seven degree-of-freedom vehicles using classical single-loop techniques, one requires decomposing the performances into sets of single-loop performances. For example the frequency response of the vehicle with respect to heave road input, roll road input, and pitch road input. For the case where road profiles induce combined heave, roll, and pitch motions, this single-loop technique may not be appropriate. Frequency responses of multiinput–multioutput systems, reflected by singular values, are required.

If the transfer functions from the  $i$ th road input  $\dot{w}_i$  to the heave, roll, and pitch accelerations are denoted as  $T_{h\dot{w}_i}(s)$ ,  $T_{r\dot{w}_i}(s)$ , and  $T_{p\dot{w}_i}(s)$ , then the following performance measure will be used to characterize BRP

$$\begin{aligned} \sigma_h(\omega) &= \bar{\sigma}(T_{h\dot{w}}(j\omega)) = \left( \sum_{i=1}^4 |T_{h\dot{w}_i}(j\omega)|^2 \right)^{1/2} \\ \sigma_r(\omega) &= \bar{\sigma}(T_{r\dot{w}}(j\omega)) = \left( \sum_{i=1}^4 |T_{r\dot{w}_i}(j\omega)|^2 \right)^{1/2} \\ \sigma_p(\omega) &= \bar{\sigma}(T_{p\dot{w}}(j\omega)) = \left( \sum_{i=1}^4 |T_{p\dot{w}_i}(j\omega)|^2 \right)^{1/2}. \end{aligned} \quad (21)$$

The WFP can be characterized by the largest and the smallest singular values of  $T_{z_{td}\dot{w}}(s)$ , which is the transfer matrix from the road input velocity vector  $\dot{w}$  to the tire deflection derivative vector

$$\dot{z}_{td} = \dot{z}_w - \dot{w}.$$

We denote them as

$$\bar{\sigma}_w(\omega) = \bar{\sigma}(T_{z_{td}\dot{w}}(j\omega))$$

$$\underline{\sigma}_w(\omega) = \underline{\sigma}(T_{z_{td}\dot{w}}(j\omega)).$$

The frequency responses are well defined in linear systems. If a system has significant nonlinearities, time responses are more appropriate for performance evaluation. A time response with respect to a frequency-sweeping time sequences could also provide certain frequency-response like characterization. For this consideration, a magnitude varying chirp signal road profile is used. This signal is shown in Fig. 4, which has frequency contents from 0 to 15 Hz. This signal for left and right side of the wheels has a frequency shift in order to excite the pitch and roll modes of the car body.

The time responses with respect to typical road profiles are also used. The actually measured road inputs are recorded data from typical road surface. In this paper a bad bump road profile

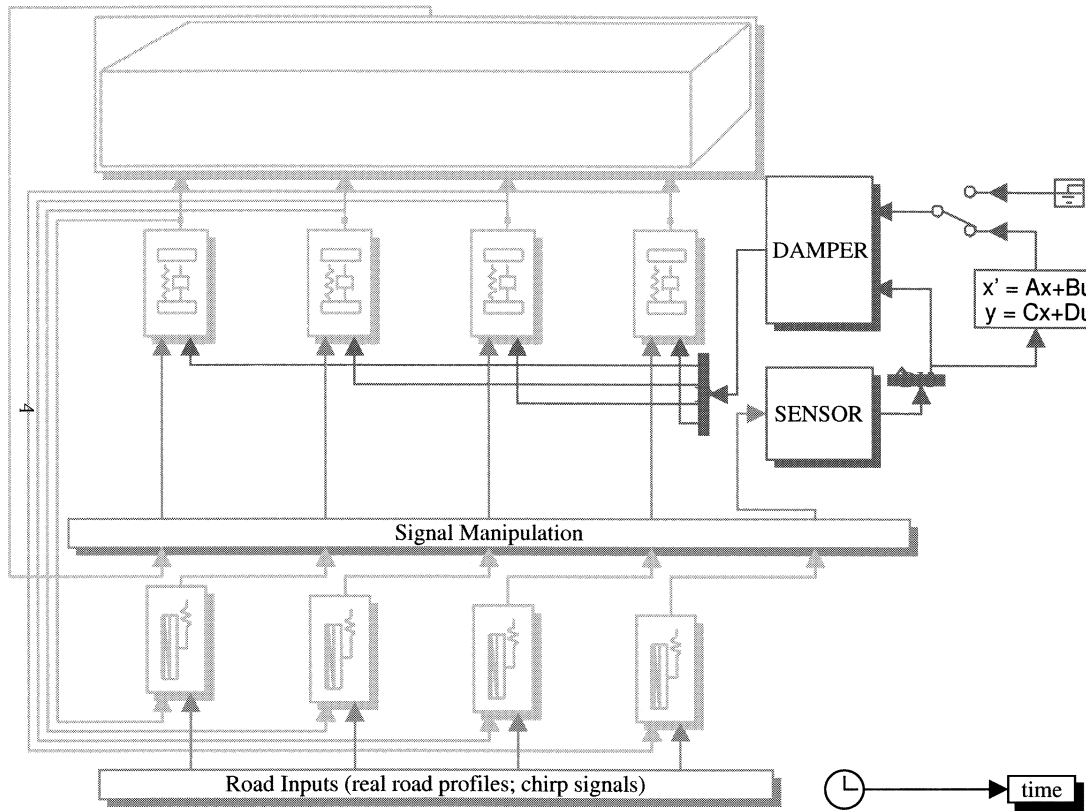


Fig. 3. Simulink model of a seven degree-of-freedom vehicle.

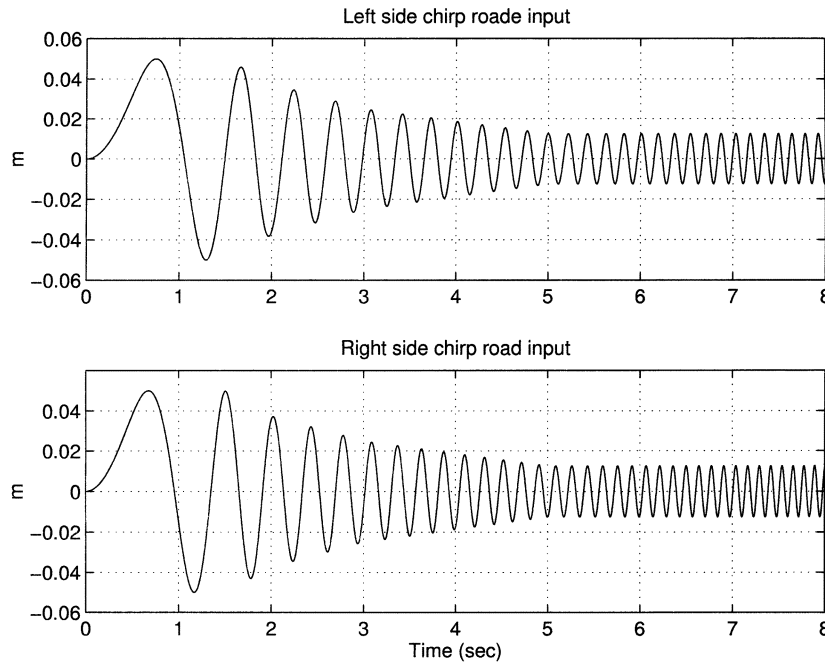


Fig. 4. Time response of the right and left road inputs.

data is used. The vehicle is assumed to travel straight in a constant speed of 60 km/h.

IV. MULTIOBJECTIVE OPTIMAL CONTROL STRATEGY

Consider the plant  $G$  described in (11)

$$\dot{x} = Ax + B_1\dot{w} + B_2u. \tag{22}$$

Let the sensor measurement be expressed as

$$y = C_yx + D_{y1}\dot{w} + D_{y2}u. \tag{23}$$

The goal here is to find an algorithm  $C$  of the following form:

$$\begin{aligned} \dot{x}_c &= A_c x_c + B_c y \\ u &= C_c x_c \end{aligned} \tag{24}$$

to limit the peak frequency responses, which is measured by the so-called  $H_\infty$  norm of the involved transfer matrix of the following variable:

$$z_\infty = C_\infty x + D_{\infty 1} \dot{w} + D_{\infty 2} u$$

and the variance of the following variable with respect to unit covariance white noise disturbance  $\dot{w}$ :

$$z_2 = C_2 x + D_{22} u.$$

The latter is also equivalent to a quadratic criterion in frequency domain and is called a  $H_2$  norm criterion.

If the loop is closed by using  $C$  to control the plant  $G$  based on the sensor signal  $y$ , then the closed-loop system can be expressed as

$$\begin{aligned} \dot{x} &= Ax + B_1 \dot{w} + B_2 u \\ z_2 &= C_2 x + D_{22} u \\ z_\infty &= C_\infty x + D_{\infty 1} \dot{w} + D_{\infty 2} u \end{aligned} \quad (25)$$

with

$$\begin{aligned} A &= \begin{bmatrix} A & B_2 C_c \\ B_c C_y & A_c + B_c D_{y2} C_c \end{bmatrix} \\ B &= \begin{bmatrix} B_1 \\ B_c D_{y1} \end{bmatrix} \\ C_2 &= [C_2 \quad D_{22} C_c] \\ C_\infty &= [C_\infty \quad D_{\infty 2} C_c] \\ D_{\infty 1} &= D_{\infty 1}. \end{aligned}$$

Denote the closed-loop transfer functions from  $\dot{w}$  to  $z_2$  in (25) as  $T_2(G, C)$  and from  $\dot{w}$  to  $z_\infty$  in (25) as  $T_\infty(G, C)$ . The  $H_2$  norm of  $T_2(G, C)$  is the following quadratic criterion, which is equivalent to the variance of the signal  $z_2$  with respect to a unit covariance white noise disturbance  $\dot{w}$

$$\|T_2(G, C)\|_2^2 = \frac{1}{2\pi} \int_{-\infty}^{\infty} \text{tr}[T_2(G, C; j\omega) T_2^*(G, C; j\omega)] d\omega$$

where  $T_2(G, C; j\omega)$  denotes the frequency response of  $T_2(G, C)$ . The  $H_\infty$  norm of  $T_\infty(G, C)$  can be computed from the following:

$$\|T_\infty(G, C)\|_\infty = \sup_w \bar{\sigma}[T_\infty(G, C; j\omega)]$$

where  $T_\infty(G, C; j\omega)$  denotes the frequency response of  $T_\infty(G, C)$ . The  $H_\infty$  norm represents the peak magnitude (peak singular value) of the frequency response of a transfer matrix. Another explanation of  $\|T_\infty(G, C)\|_\infty$  is the square root of the energy amplification factor of  $z_\infty$  with respect to all possible inputs  $\dot{w}$

$$\|T_\infty(G, C)\|_\infty^2 = \max_{\dot{w}} \left\{ \frac{\int_0^\infty z_\infty'(t) z_\infty(t) dt}{\int_0^\infty \dot{w}'(t) \dot{w}(t) dt} : \dot{w} \text{ has nonzero but finite energy} \right\}.$$

TABLE I  
SUMMARY OF THE VEHICLE PARAMETERS

$M_s$ (kg)	$I_{xx}$ (kgm <sup>2</sup> )	$I_{yy}$ (kgm <sup>2</sup> )	
1583	531	2555	
$M_{w1}$ (kg)	$M_{w2}$ (kg)	$M_{w3}$ (kg)	$M_{w4}$ (kg)
48	48	74	74
$K_{s1}$ (N/m)	$K_{s2}$ (N/m)	$K_{s3}$ (N/m)	$K_{s4}$ (N/m)
35000	35000	34000	34000
$C_{s1}$ (Ns/m)	$C_{s2}$ (Ns/m)	$C_{s3}$ (Ns/m)	$C_{s4}$ (Ns/m)
400	400	200	200
$K_{t1}$ (Ns/m)	$K_{t2}$ (Ns/m)	$K_{t3}$ (Ns/m)	$K_{t4}$ (Ns/m)
220000	220000	220000	220000
$l_{zf}$ (m)	$l_{zr}$ (m)		
1.116	1.438		
$l_{yf}$ (m)	$l_{yr}$ (m)	$l_{yr}$ (m)	$l_{yr}$ (m)
0.77	0.77	0.765	0.765

TABLE II  
SUMMARY OF THE PASSIVE SUSPENSION PERFORMANCE

$\ T_\infty(G, 0)\ _\infty$	17.95
Front: $\ T_{\infty 1}(G, 0)\ _\infty$	7.41
Rear: $\ T_{\infty 3}(G, 0)\ _\infty$	17.83
$\ T_2(G, 0)\ _2$	90.85
Heave: $\ T_{21}(G, 0)\ _2$	40.41
Roll: $\ T_{22}(G, 0)\ _2$	72.11
Pitch: $\ T_{23}(G, 0)\ _2$	32.97

The  $H_\infty$  norm of  $T_\infty(G, C)$  does not exceed a given performance level  $\gamma_\infty$  if and only if there exists a

$$P = P' > 0$$

such that the following linear matrix inequality is true [6], [18]:

$$\begin{bmatrix} AP + PA' & B & PC'_\infty \\ B' & -I & D'_\infty \\ C_\infty P & D_\infty & -\gamma_\infty^2 I \end{bmatrix} < 0. \quad (26)$$

The  $H_2$  norm of  $T_2(G, C)$  does not exceed a given performance level  $\gamma_2 > 0$  if and only if there exists a

$$Q = Q' > 0$$

such that the following linear matrix inequality is true:

$$\begin{bmatrix} AQ + QA' & B \\ B' & -I \end{bmatrix} < 0 \quad (27)$$

$$\text{tr}[C_2 Q C_2'] < \gamma_2^2. \quad (28)$$

Finding a  $C$  to satisfy (26) or (28) can be solved by the well-known  $H_\infty$  control or  $H_2$  control theory. However, finding a controller  $C$  to simultaneously satisfy (26) and (28) is still an

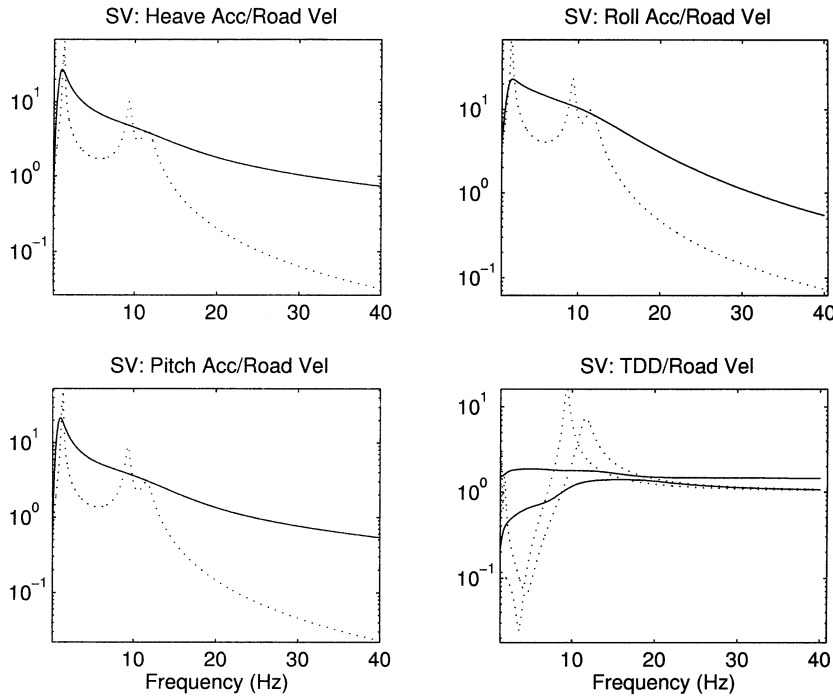


Fig. 5. Frequency response for the body heave, roll, and pitch accelerations with respect to road velocity inputs. Frequency response for tire deflection derivatives. Dotted line: passive, solid line: active controller  $C^w$ .

TABLE III  
SUMMARY OF THE PERFORMANCE USING THE WFP-EMPHASIZED  
CONTROLLER  $C^w$

$\ T_\infty(G, C^w)\ _\infty$	1.48
Front: $\ T_{\infty 1}(G, C^w)\ _\infty$	1.11
Rear: $\ T_{\infty 3}(G, C^w)\ _\infty$	1.41
$\ T_2(G, C^w)\ _2$	100.09
Heave: $\ T_{21}(G, C^w)\ _2$	52.89
Roll: $\ T_{22}(G, C^w)\ _2$	74.36
Pitch: $\ T_{23}(G, C^w)\ _2$	41.11

open problem and it may be computationally intractable. For computational tractability, a single Lyapunov matrix

$$X \triangleq P = Q$$

is sought in the above conditions, see [9] for detail. This simplification leads to a performance upper bound for both  $H_2$  and  $H_\infty$  norms of the closed-loop system (25). Denote the corresponding upper bounds for  $\|T_2(G, C)\|_2$  and  $\|T_\infty(G, C)\|_\infty$  as

$$\overline{\|T_2(G, C)\|_2}, \quad \overline{\|T_\infty(G, C)\|_\infty}.$$

The recently well-studied mixed  $H_2/H_\infty$  control theory finds controllers such that those upper bounds are optimized or constrained.

*Mixed  $H_2/H_\infty$  Control Problem:* For a given plant  $G$ , solve for an active controller  $C$  from any of the following optimization

problems for given performance level  $\gamma_2$ ,  $\gamma_\infty$ , or weight pair  $(\alpha, \beta)$

$$J_1 = \min_C \left\{ \overline{\|T_\infty(G, C)\|_\infty} : \overline{\|T_2(G, C)\|_2} \leq \gamma_2 \right\}$$

$$J_2 = \min_C \left\{ \overline{\|T_2(G, C)\|_2} : \overline{\|T_\infty(G, C)\|_\infty} \leq \gamma_\infty \right\}$$

$$J_3 = \min_C \left[ \alpha \overline{\|T_2(G, C)\|_2} + \beta \overline{\|T_\infty(G, C)\|_\infty} \right].$$

By using the linear matrix inequality solver (for example, LMI control toolbox associated with Matlab), the solutions for the above problem can be found, see [9]. This problem is transferred to a convex optimization problem and globally optimal controller can be found.

Notice that the performance bounds  $\gamma_\infty$  or  $\gamma_2$  is required to be feasible in order to have a solution for the mixed  $H_2/H_\infty$  control problem. Hence, the choice of those bounds are very important in shaping the performances of the final closed-loop systems.

Since  $z_\infty$  and  $z_2$  are both vector variables, the performance achieved by the optimal controller might not reflect the performance for the individual variables. We are really interested in each element in  $z_\infty$  and  $z_2$ . The following variable normalization uses the corresponding open-loop norms to weight the corresponding contributions of the individual variables in total  $H_2$  and  $H_\infty$  norms. Let  $z_{2i} \in \mathbb{R}$  be the  $i$ th element of  $z_2$ , and  $z_{\infty i} \in \mathbb{R}$  be the  $i$ th element of  $z_\infty$ . Denote the transfer function from  $\dot{w}$  to  $z_{\infty i}$  as  $T_{\infty i}(G, C)$  for  $i = 1, 2, \dots, m$ , and from  $\dot{w}$  to  $z_{2i}$  as  $T_{2i}(G, C)$  for  $i = 1, 2, \dots, n$ . Assume the plant  $G$  is stable, i.e., the open-loop transfer functions

$$T_{\infty i}(G, 0), \quad T_{2i}(G, 0)$$



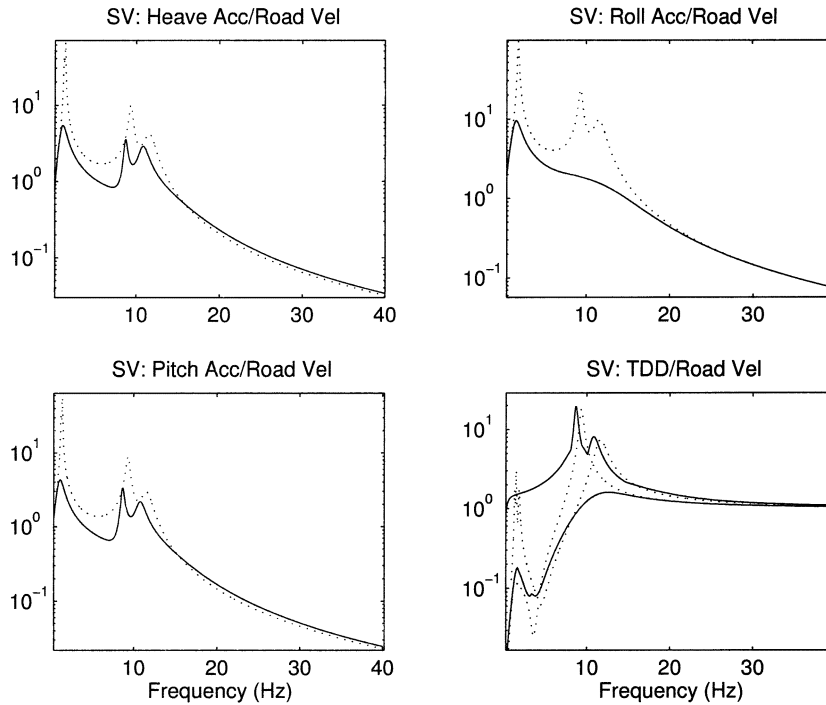


Fig. 6. Frequency response of heave, roll, and pitch accelerations, and one tire deflection derivative. Dotted lines: passive, solid line: active controller  $C^b$ .

TABLE IV  
SUMMARY OF THE PERFORMANCE USING THE BRP-EMPHASIZED  
CONTROLLER  $C^b$

$\ T_\infty(G, C^b)\ _\infty$	19.33
Front: $\ T_{\infty 1}(G, C^b)\ _\infty$	5.9
Rear: $\ T_{\infty 3}(G, C^b)\ _\infty$	14.28
$\ T_2(G, C^b)\ _2$	23.70
Heave: $\ T_{21}(G, C^b)\ _2$	11.30
Roll: $\ T_{22}(G, C^b)\ _2$	18.80
Pitch: $\ T_{23}(G, C^b)\ _2$	8.99

have finite  $H_\infty$  and  $H_2$  norms.

The  $i$ th normalized variable for the  $i$ th element of  $z_\infty$  is defined as

$$\tilde{z}_{\infty i} = \frac{C_{\infty i}}{\|T_{\infty i}(G, 0)\|_\infty} x + \frac{D_{\infty i}}{\|T_{\infty i}(G, 0)\|_\infty} w + \frac{D_{\infty 2i}}{\|T_{\infty i}(G, 0)\|_\infty} u$$

or equivalently, we are dealing with the following transfer matrix in the mixed  $H_2/H_\infty$  control problem:

$$\tilde{T}_\infty(G, C) \triangleq \text{diag} \left( \frac{1}{\|T_{\infty 1}(G, 0)\|_\infty}, \dots, \frac{1}{\|T_{\infty m}(G, 0)\|_\infty} \right) \cdot T_\infty(G, C).$$

Similarly, the  $i$ th normalized variable for the  $i$ th element of  $z_2$  is defined as

$$\tilde{z}_{2i} = \frac{C_{2i}}{\|T_{2i}(G, 0)\|_2} x + \frac{D_{2i}}{\|T_{2i}(G, 0)\|_2} w + \frac{D_{22i}}{\|T_{2i}(G, 0)\|_2} u$$

or equivalently, we are dealing with the following transfer matrix in the mixed  $H_2/H_\infty$  control problem:

$$\tilde{T}_2(G, C) \triangleq \text{diag} \left( \frac{1}{\|T_{21}(G, 0)\|_2}, \dots, \frac{1}{\|T_{2n}(G, 0)\|_2} \right) \cdot T_2(G, C).$$

Let us now choose the  $H_\infty$  and  $H_2$  performance variables in the suspension control design. Consider the seven degree-of-freedom vehicle model shown in Fig. 1. The ride control performance BRP aims to reduce the acceleration levels of the car body on almost the whole frequency range, i.e., good vibration isolation. As we know for the quarter-car model, there is an invariant point (frequency) where the magnitude of the involved frequency response can not be affected by active controllers. Since  $H_\infty$  norm optimization wants to limit the peak value of the frequency response, this invariant point becomes a major barrier for the achievable performance in control design. By using a quarter-car model [13] actually showed that the controller designed for  $H_\infty$  performance did not achieve good ride performance at all. Therefore, it is not reasonable to characterize the BRP performance using  $H_\infty$  norm. Also [11], [12] support root mean square (rms) or  $H_2$ -type of performance metric for BRP. We characterize BRP by the  $H_2$  norm for the following variable:

$$z_2 = \ddot{q} = \begin{bmatrix} \ddot{h} \\ \ddot{r} \\ \ddot{p} \end{bmatrix}.$$

On the other hand, the wheel control performance aims to reduce the wheel dynamic normal force. That is, we would like to keep the magnitude of the frequency response of the involved

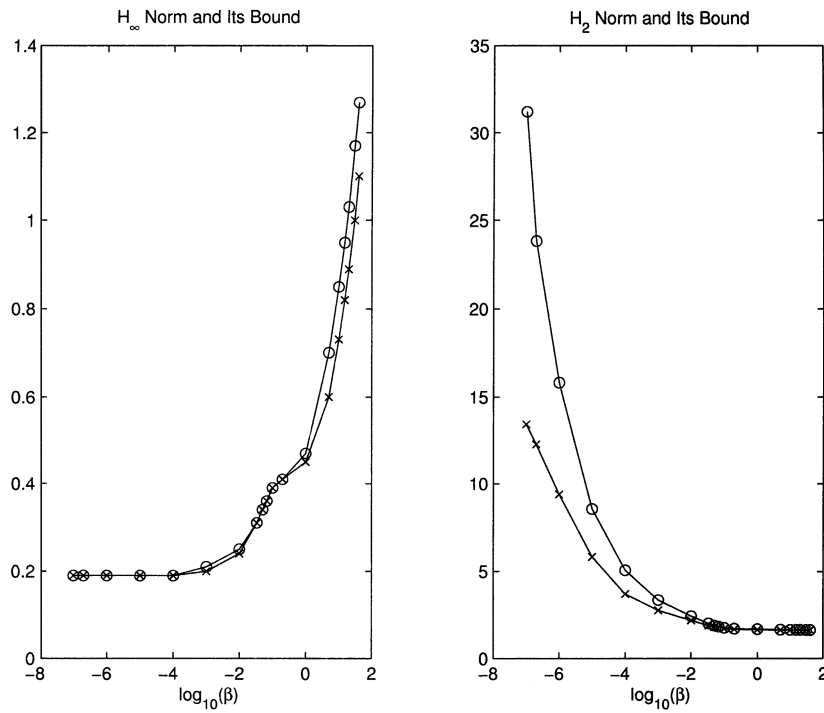


Fig. 7.  $H_2$  and  $H_\infty$  norms and their upper bounds at each control design.

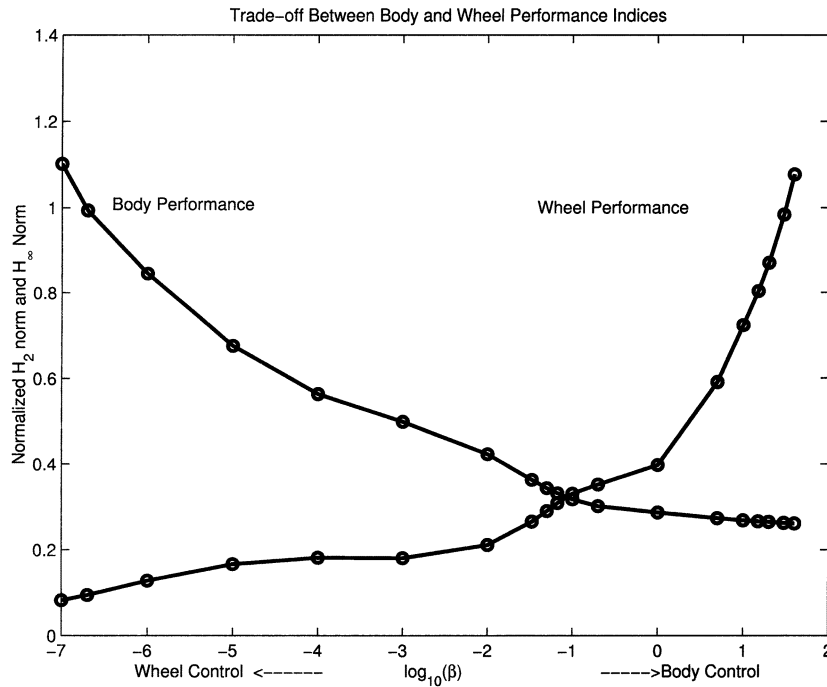


Fig. 8. Tradeoff between body and wheel performance.

transfer function as constant as possible within all the frequency region. Hence, an  $H_\infty$  norm performance for WFP is appropriate and we define

$$z_\infty = \dot{z}_{td} = \dot{z}_w - \dot{w}.$$

The sensors used here are the relative position sensors, which measure  $z_{rp}$ . Note that  $z_{rp}$  includes the steady-state portion of

the displacements due to static sprung mass or the dead load. In order to remove this steady-state offset, a high-pass filter can be used. However, in this paper, the time derivative  $\dot{z}_{rp}$  is used. That is, instead of feeding back the high-pass-filtered  $z_{rp}$  to the control algorithm,  $\dot{z}_{rp}$  is used. Both hardware differentiation and software differentiation can be used to obtain  $\dot{z}_{rp}$  from  $z_{rp}$ . Hence, the measurement for control algorithms is

$$y = \dot{z}_{rp}. \tag{29}$$

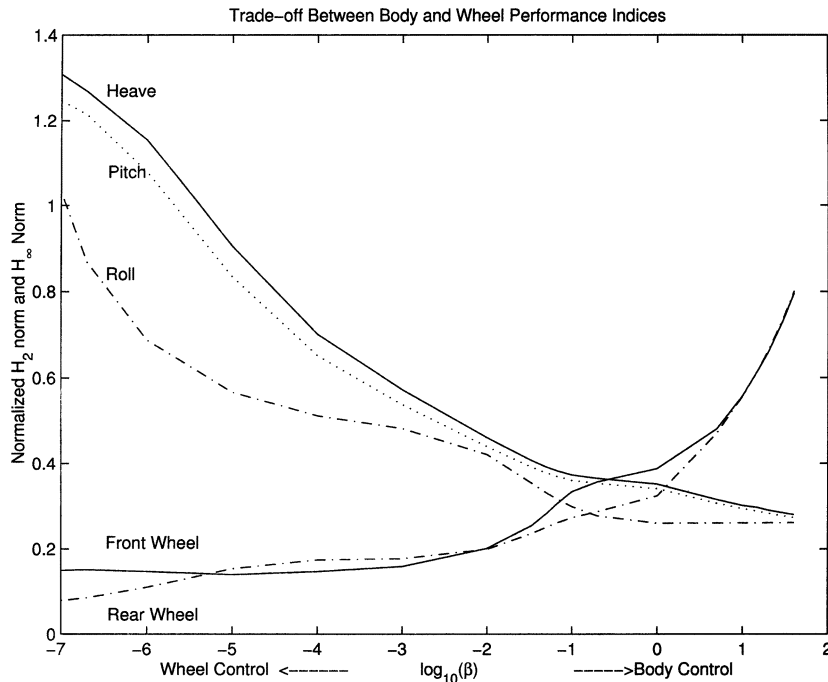


Fig. 9. Tradeoff between body heave, roll, and pitch accelerations, and the front- and rear-wheel tire deflection derivatives.

TABLE V  
SUMMARY OF THE PERFORMANCE USING THE BALANCED CONTROLLER  $C^{bw}$

$\ T_{\infty}(G, C^{bw})\ _{\infty}$	14.42
Front: $\ T_{\infty 1}(G, C^{bw})\ _{\infty}$	4.56
Rear: $\ T_{\infty 3}(G, C^{bw})\ _{\infty}$	10.98
$\ T_2(G, C^{bw})\ _2$	24.16
Heave: $\ T_{21}(G, C^{bw})\ _2$	11.89
Roll: $\ T_{22}(G, C^{bw})\ _2$	18.77
Pitch: $\ T_{23}(G, C^{bw})\ _2$	9.47

Using the system state  $x$ ,  $y$  can be expressed as in (23) with

$$C_y = [0 \ 0 \ H \ -I]$$

$$D_{y1} = C_y N$$

$$D_{y2} = 0.$$

## V. NUMERICAL EXAMPLE

Consider the seven degree-of-freedom vehicle depicted in Fig. 1. The vehicle parameters are summarized in Table I. The  $H_2$  and  $H_{\infty}$  norms of the corresponding transfer matrices for the passive suspensions can be computed as in Table II.

The control goal here is to compute the active control signal  $u$ , based on the sensor measurement  $y$  defined in (29), such that the following cost function for a fixed  $\beta$  is minimized:

$$J(\beta) = \min_C \left[ \|\tilde{T}_{\infty}(G, C)\|_{\infty} + \beta \|\tilde{T}_2(G, C)\|_2 \right] \quad (30)$$

where the normalized transfer matrices are

$$\tilde{T}_{\infty}(G, C) \triangleq \text{diag} \left( \frac{1}{7.41}, \frac{1}{7.41}, \frac{1}{17.83}, \frac{1}{17.83} \right) T_{\infty}(G, C)$$

$$\tilde{T}_2(G, C) \triangleq \text{diag} \left( \frac{1}{40.41}, \frac{1}{72.11}, \frac{1}{32.97} \right) T_2(G, C).$$

Notice that for small  $\beta$ , the optimal controller tries to suppress the peak values in the frequency responses for the wheel performance with less concern for the body performance. A controller corresponding to small  $\beta$  should be called a WFP-emphasized controller, denote it as  $C^w$ . One of such controllers is the one corresponding to  $\beta = 10^{-7}$ . Fig. 5 shows the singular values of the heave, roll, and pitch acceleration transfer functions with respect to the road profile velocities. It can be seen that although the peak values of the transfer function of the tire deflection derivatives are reduced, the body acceleration levels are actually increased significantly over the passive suspension in almost all the frequency region. That is, the good wheel performance is achieved in the expense of the ride performance. This result is consistent with the nature of the wheel emphasized performance. Table III summarizes the performance indexes corresponding to controller  $C^w$ .

For large  $\beta$ , the controller tries to reduce the  $H_2$  norm for the body heave, roll, and pitch accelerations. We should call this BRP-emphasized controller. One of such controllers is the one corresponding to  $\beta = 40$ , denoted as  $C^b$ . Fig. 6 shows that the frequency response of the heave, roll, and pitch accelerations are reduced dramatically in comparison with the passive suspension. However, the tire deflection derivative frequency responses even get worse than the passive suspension. That is, the good body performance is achieved in the expense of the wheel performance. Table IV summarizes the performance indexes for controller  $C^b$ . An invariant point (see [10] for definition) in frequency response for both pitch and heave motions can be found, where both active and passive suspension share the same magnitude for their singular values. Notice that this is not necessarily true for the roll motion. Further study is needed in order to explain this.

The above control designs correspond to two extreme  $\beta$ s, which shows potential tradeoffs between BRP and WFP. In

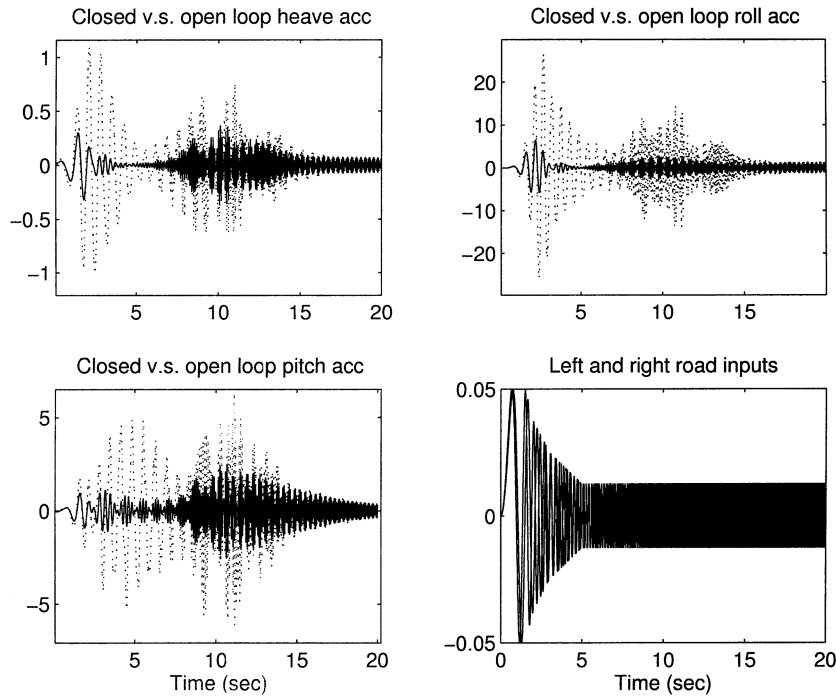


Fig. 10. Time response of the body heave, roll, and pitch with respect to chirp road inputs. Dotted line: passive, solid lines: active controller  $C^{bw}$ .

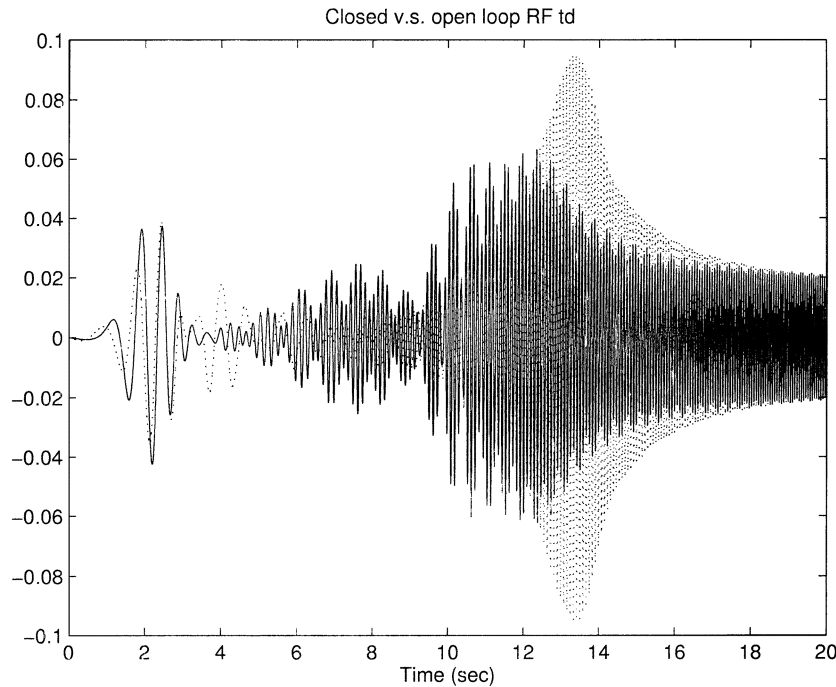


Fig. 11. Time response of the tire deflection derivatives with respect to chirp road inputs. Dotted line: passive, solid lines: active controller  $C^{bw}$ .

order to conduct such tradeoff, 19  $\beta$ s between  $\beta = 10^{-7}$  and  $\beta = 40$  have been chosen as follows:

$$\beta_{1\dots5} = \left[ 10^{-7} \quad \frac{10^{-6}}{5} \quad 10^{-6} \quad 10^{-5} \quad 10^{-4} \right]$$

$$\beta_{6\dots10} = \left[ 10^{-3} \quad 10^{-2} \quad \frac{1}{30} \quad \frac{1}{20} \quad \frac{1}{15} \right]$$

$$\beta_{11\dots19} = \left[ \frac{1}{10} \quad \frac{1}{5} \quad 1 \quad 5 \quad 10 \quad 15 \quad 20 \quad 30 \quad 40 \right]$$

and 19 controllers  $C_i$ s ( $i = 1, 2, \dots, 19$ ) corresponding to those  $\beta$ s have been designed using LMI control toolbox in Matlab [9], where

$$C_1 = C^w$$

and

$$C_{19} = C^b.$$

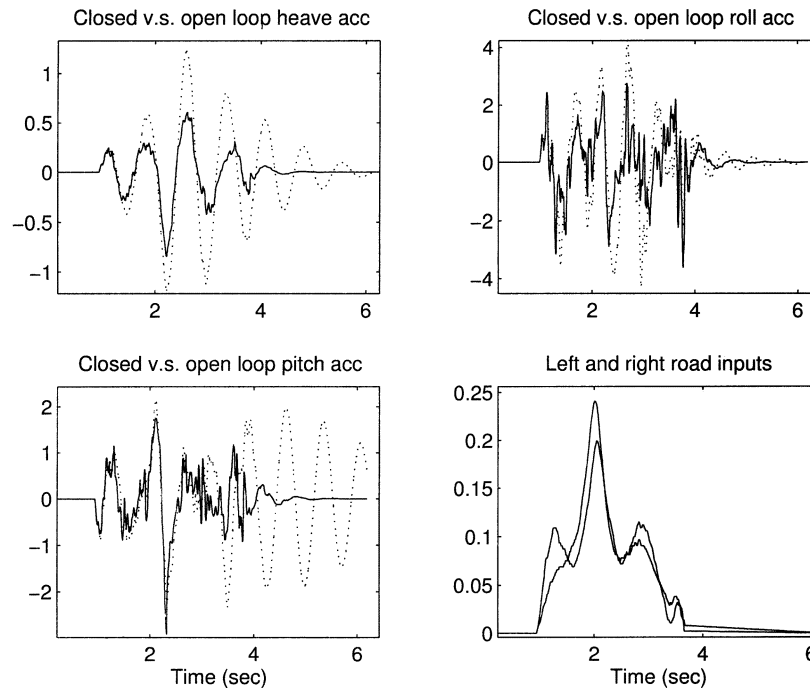


Fig. 12. Body heave, roll, and pitch acceleration with respect to bad bump road inputs. Dotted line: passive; solid line: semiactive.

The norms  $\|\tilde{T}_2(G, C_i)\|_2$  and  $\|\tilde{T}_\infty(G, C_i)\|_\infty$ , and their upper-bounds for  $i = 1, 2, \dots, 19$  are shown in Fig. 7. From this figure, it can be found that increasing  $\beta$  implies increasing the  $H_\infty$  norm and decreasing the  $H_2$  norm.

The actual  $H_2$  and  $H_\infty$  norms of the controlled suspensions are our main concerns, for  $i = 1, 2, \dots, 19$ , we plot

$$\frac{\|T_\infty(G, C_i)\|_\infty}{\|T_\infty(G, 0)\|_\infty}, \quad \frac{\|T_2(G, C_i)\|_2}{\|T_2(G, 0)\|_2}$$

with respect to  $\beta_i$  in Fig. 8. From this figure, it is not hard to find that there exist some  $\beta$ s such that both BRP and WFP could achieve reasonable levels. The weighted transfer functions take care of the relative importance of the individual variables in the total cost defined in (30), the achieved heave, roll, and pitch accelerations, and the front and the rear tire deflection derivatives should obey the similar trends. This individual performance trends can be found in Fig. 9.

A controller corresponding to  $\beta = 15$  is chosen as the balanced controller, we denote this controller as  $C^{bw}$ . This controller achieves the performances summarized in Table V.

The frequency responses of the closed-loop systems corresponding to  $C^{bw}$  can be similarly constructed as for controllers  $C^w$  and  $C^b$  for linear dynamics. The frequency responses could also be seen for nonlinear vehicle dynamics by using the time response with respect to a frequency sweeping signal. What we used here is the varying magnitude chirp signal defined in Section III. In order to conduct time domain simulation, a simulink model of seven degrees of freedom with nonlinear suspension characterizations, developed at Delphi Automotive Systems has been used (see Fig. 3). The time response simulated with respect to the magnitude varying chirp signal described in Section III are shown in Figs. 10 and 11. From the responses we can find that  $C^{bw}$  generally does a good job in reducing the peak value

of the heave, roll, and pitch in all the frequency range. The controller has an appealing feature of reducing the peak values in middle frequency range (from 4 to 8 Hz) and a very good roll performance. The tire deflection derivative frequency response shows reduction on the peak value around wheel hop frequency (around 10 Hz).

In the semiactive damper case, the control force is realized by a damper. The resultant damper force is nonlinear function of the demand active control force  $u$  and the relative velocity  $\dot{z}_{rp}$ . If we denote this nonlinear function as  $f(\cdot)$ , then the total suspension force can be written as

$$S(u, z_{rp}, \dot{z}_{rp}) = -K_s z_{rp} - C_s \dot{z}_{rp} + f(u, \dot{z}_{rp}).$$

We use the time response with proper damper characterization to evaluate the balanced controller  $C^{bw}$ . The road profile input used here is the bad bump road profile, which is used in vehicle model developed at Delphi Automotive Systems. The vehicle time responses is shown in Figs. 12 and 13. The vehicle achieves good performance for heave and pitch accelerations. Due to the fact that the damping in the system is added appropriately, both body and wheel vibrations are attenuated very fast. From Figs. 12 and 13, we can find that as soon as the vehicle passes the bump, the vibration of the tire deflection completely disappears, while the body vibrations take another 0.5 s to completely disappear.

## VI. CONCLUSION

The matrix form of seven degree-of-freedom vertical vehicle dynamics model simplifies the derivation of equations of motions and provides insight about the system states. Using a linear transformation, the original seven degree-of-freedom equation of motion with road input  $w$  as disturbance can be transformed to the one using road input velocity  $\dot{w}$  as

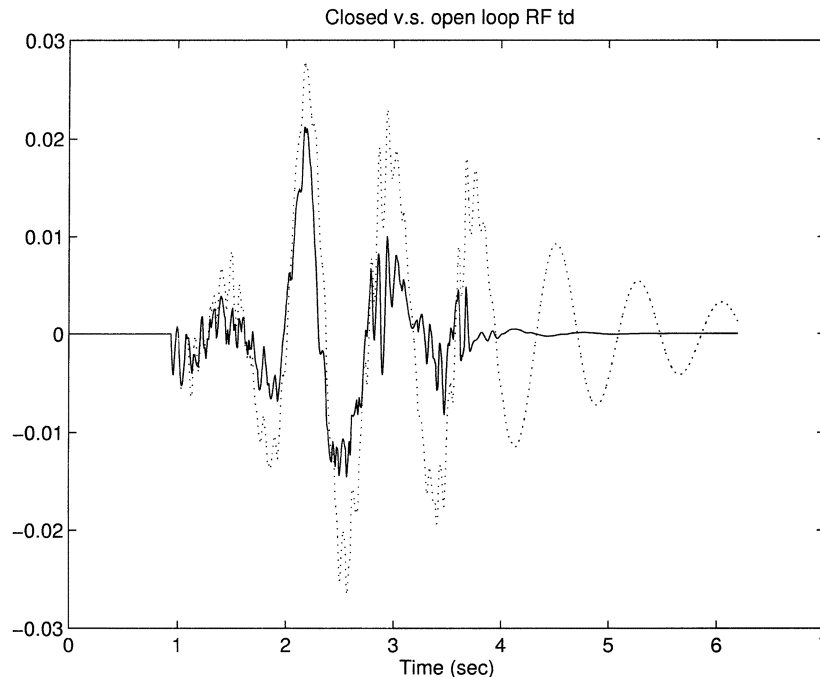


Fig. 13. Time response of the tire deflection with respect to bad bump road inputs. Dotted line: passive; solid line: semiactive.

disturbance. This transformed seven degree-of-freedom vehicle model are used to design an active suspension to simultaneously achieve the  $H_2$  performance for the body accelerations and the  $H_\infty$  performance of the tire deflection derivatives. The  $H_\infty$  norm is a good measure of wheel performance but may not be a good measure of the body performance. The balanced control law, which achieves both body and wheel performance by trading off between BRP and WFP, are then validated through simulation and applied to semiactive suspensions. The simulation results show that the control law thus designed achieves better performance than many existing controllers for full car models, which are mainly dealing with the ride performances. As a by-product, our example shows that the invariant point in the quarter model case exists in the seven degree-of-freedom model for heave and pitch motion but are not necessarily true for roll motion. The future work will focus on the extension of this work to integrated vehicle dynamics control.

#### ACKNOWLEDGMENT

The authors wish to thank Dr. R. Longhouse and Dr. A. Hac, Delphi Automotive Systems, for discussions which were valuable to the completion of the work, and Dr. D. Hrovat at Ford Motor Company for reading the draft of this paper and constructive suggestions.

#### REFERENCES

- [1] A. Alleyne and J. K. Hedrick, "Adaptive control for active suspension," *ASME Advanced Automotive Technol.*, vol. 52, pp. 7–13, 1993.
- [2] M. B. A. Abdel-Hardy and D. A. Crolla, "Theoretical analysis of active suspension performance using a four-wheel model," *Proc. Inst. Mech. Eng.*, vol. 203(D), pp. 125–135, 1989.
- [3] —, "Active suspension control algorithms for a fourwheel vehicle model," *Int. J. Vehicle Design*, vol. 13, no. 2, pp. 144–158, 1992.
- [4] P. Barak, "On a ride control algorithm for heave, pitch and roll motions of a motor vehicle," Ph.D. dissertation, Dept. Mech. Eng., Wayne State Univ., Detroit, MI, 1985.
- [5] D. S. Bernstein and W. M. Haddad, "LQG control with an  $H_\infty$  performance bound: A Riccati equation approach," *IEEE Trans. Automat. Contr.*, vol. 34, p. 293, Feb. 1989.
- [6] S. Boyd, L. E. Ghaoui, E. Feron, and V. Balakrishnan, *Linear Matrix Inequality Syst. Contr. Theory*. Philadelphia, PA: SIAM, 1995.
- [7] P. Barak and D. Hrovat, "Application of the LQG approach to design of an automotive suspension for three dimensional vehicle models," in *Proc. Int. Conf. on Advanced Suspensions*. London, U.K.: IMECHE, 1988.
- [8] R. M. Chalasani, "Ride performance potential of active suspension systems—Part II: Comprehensive analysis based on a full-car model," presented at the ASME Symp. Simulation Ground Vehicles Transportation Syst., Anaheim, CA, 1986.
- [9] P. Gahinet, A. Nemirovski, A. J. Laub, and M. Chilali, *LMI Control Toolbox for Use With Matlab*. Natick, MA: The Mathworks Inc., 1995.
- [10] J. K. Hedrick and T. Butsuen, "Invariant properties of automotive suspensions," presented at the IMechE Conf. Advanced Suspensions, London, U.K., 1988.
- [11] D. Hrovat, "Application of optimal control to advanced automotive suspension design," *ASME J. Dyn. Syst., Measurement, Contr.*, pp. 328–342, 1993.
- [12] —, "Survey of advanced suspension developments and related optimal control applications," *Automatica*, pp. 1781–1816, 1997.
- [13] A. G. DeJager, "Comparison of two methods for the design of active suspension systems," *Optimal Contr. Applicat. Methods*, vol. 12, pp. 173–188, 1991.
- [14] H. A. Hindi, B. Hassibi, and S. P. Boyd, "Multiobjective  $H_2/H_\infty$ -Optimal control via finite dimensional Q-parameterization and linear matrix inequalities," in *Proc. Amer. Contr. Conf.*, 1998, pp. 3244–3248.
- [15] T. Hirata, S. Koizumi, and R. Takahashi, " $H_\infty$  control of railroad vehicle active suspension," *Automatica*, pp. 13–24, 1995.
- [16] P. P. Khargonekar and M. Rotea, "Mixed  $H_2/H_\infty$  control: A convex optimization approach," *IEEE Trans. Automat. Contr.*, vol. 36, pp. 824–837, 1991.
- [17] D. Mustafa, "Relations between maximum entropy/ $H_\infty$  control and combined  $H_\infty$ /LQG control," *Syst. Contr. Lett.*, vol. 12, p. 193, 1989.
- [18] R. E. Skelton, T. Iwasaki, and K. Grigoriadis, *A Unified Algebraic Approach to Control Design*. London, U.K.: Taylor and Francis, 1997.
- [19] R. H. Takahashi, J. F. Camino, D. E. Zampieri, and P. L. D. Peres, "A multiobjective approach for  $H_2$  and  $H_\infty$  active suspension control," in *Proc. Amer. Contr. Conf.*, vol. 1, 1998, pp. 48–52.



**Jianbo Lu** (S'93–M'97) received the M.S.M.E. degree from Arizona State University, Tempe, and the Ph.D. degree in aerospace engineering from Purdue University, West Lafayette, IN.

From 1986 to 1990, he was an Engineer at China Academy of Railway Sciences. From 1997 to 2000, he was with Delphi Automotive Systems. In May 2000, he joined Ford Motor Company, where he is currently involved in research and development for advanced automotive controls.

Dr. Lu is a Member of ASME and Tau Beta Pi. He received the Henry Ford Technology Award, the highest technical achievement award at Ford Motor Company, for his contributions in vehicle dynamics and controls, in September 2002.

**Mark DePoyster** is currently a Chief Engineer, Advanced Chassis Control Engineering, Engine Management and Chassis Systems, Delphi Automotive Systems.